Molecular Cell
Article

circRNA Biogenesis Competes with Pre-mRNA Splicing

Reut Ashwal-Fluss,[1,3] Markus Meyer,[2,3] Nagarjuna Reddy Pamudurti,[1,3] Andranik Ivanov,[2] Osnat Bartok,[1] Mor Hanan,[1] Naveh Evantal,[1] Sebastian Memczak,[2] Nikolaus Rajewsky,[2,*] and Sebastian Kadener[1,*]
[1]Biological Chemistry Department, Silberman Institute of Life Sciences, The Hebrew University of Jerusalem, Jerusalem 91904, Israel
[2]Systems Biology of Gene Regulatory Elements, Max-Delbrück-Center for Molecular Medicine, Berlin 13092, Germany
[3]Co-first author
*Correspondence: rajewsky@mdc-berlin.de (N.R.), skadener@mail.huji.ac.il (S.K.)
http://dx.doi.org/10.1016/j.molcel.2014.08.019

SUMMARY

Circular RNAs (circRNAs) are widely expressed noncoding RNAs. However, their biogenesis and possible functions are poorly understood. Here, by studying circRNAs that we identified in neuronal tissues, we provide evidence that animal circRNAs are generated cotranscriptionally and that their production rate is mainly determined by intronic sequences. We demonstrate that circularization and splicing compete against each other. These mechanisms are tissue specific and conserved in animals. Interestingly, we observed that the second exon of the splicing factor *muscleblind* (MBL/MBNL1) is circularized in flies and humans. This circRNA (circMbl) and its flanking introns contain conserved *muscleblind* binding sites, which are strongly and specifically bound by MBL. Modulation of MBL levels strongly affects circMbl biosynthesis, and this effect is dependent on the MBL binding sites. Together, our data suggest that circRNAs can function in gene regulation by competing with linear splicing. Furthermore, we identified *muscleblind* as a factor involved in circRNA biogenesis.

INTRODUCTION

Circular RNAs (circRNAs) are unusually stable RNAs produced by circularization of exons through a poorly characterized mechanism (Capel et al., 1993; Hansen et al., 2013; Memczak et al., 2013; Salzman et al., 2012, 2013; Jeck et al., 2013). Two of them, CDR1as/ciRS-7 and *Sry,* can act as miRNA sponges (Hansen et al., 2013; Memczak et al., 2013), but no function is known for the other thousands of circRNAs that have been found across the animal kingdom (Danan et al., 2012; Hansen et al., 2013; Jeck et al., 2013; Memczak et al., 2013; Salzman et al., 2012, 2013; Wang et al., 2014). Since CDR1as is an extreme case with > 70 miRNA binding sites, we and others have speculated that circRNAs may have other functions, for example, they could be involved in protein and/or RNA transport, they could be involved in complex assembly, or they could act in *trans* (Memczak et al., 2013). It has been argued that circRNA expression levels cannot be generally explained by simple correlation with the expression of their linear isoforms (Salzman et al., 2013), indicating a potentially widespread layer of previously unknown gene regulation. Most circRNAs are hosted by protein coding genes and contain complete exons, which indicates that RNA polymerase II (RNA pol II) transcribes them and that their biogenesis is likely mediated by the spliceosome. In vitro experiments show that the splicing machinery can circularize exons (Braun et al., 1996; Pasman et al., 1996). Moreover, in the majority of cases canonical splice sites precisely flank head-to-tail junctions of circular transcripts. Exons that generate circRNAs are typically not alternatively spliced (Jeck et al., 2013; Salzman et al., 2012). Thus, circRNAs are typically generated at the expense of canonical mRNA isoforms, which can be much less abundant than the circRNAs they host (Salzman et al., 2012). This suggests that circRNA biogenesis per se might be an important regulator of mRNA production.

Most RNA pol II transcripts are capped, spliced, and polyadenylated cotranscriptionally (for review see Bentley, 2014). The carboxyl-terminal domain (CTD) of RNA pol II coordinates RNA synthesis and pre-mRNA processing (Bentley, 2014) events by direct interaction between the CTD and pre-mRNA processing factors (i.e., capping and splicing factors [Bentley, 2014]). RNA pol II can also influence pre-mRNA processing through changes in the transcription elongation rate, a well-characterized modulator of alternative splicing (Kornblihtt et al., 2013). Although well coordinated, RNA-processing events can compete with each other as in alternative splicing, cleavage, and polyadenylation in intronic regions (Kaida et al., 2010; Zhao and Manley, 1996) and synthesis of pre-miRNAs located at intron-exon junctions (Melamed et al., 2013).

It has been shown that circRNA-forming exons are often bracketed by unusually long introns in which splicing is thought to be less efficient. Moreover, these introns in humans are enriched in ALU repeats (Jeck et al., 2013), and in the single case of the *Sry* circRNA it has been shown that intronic elements can be sufficient to promote circularization (Dubin et al., 1995). However, these introns contain almost perfect complementary regions of 15 kb on either side of the SRY circRNA, which is highly exceptional. In summary, there are links between splicing and circRNA biogenesis, but it is still unknown whether circRNAs are generated cotranscriptionally or posttranscriptionally and which *cis*- or *trans*-acting factors can regulate exon circularization.

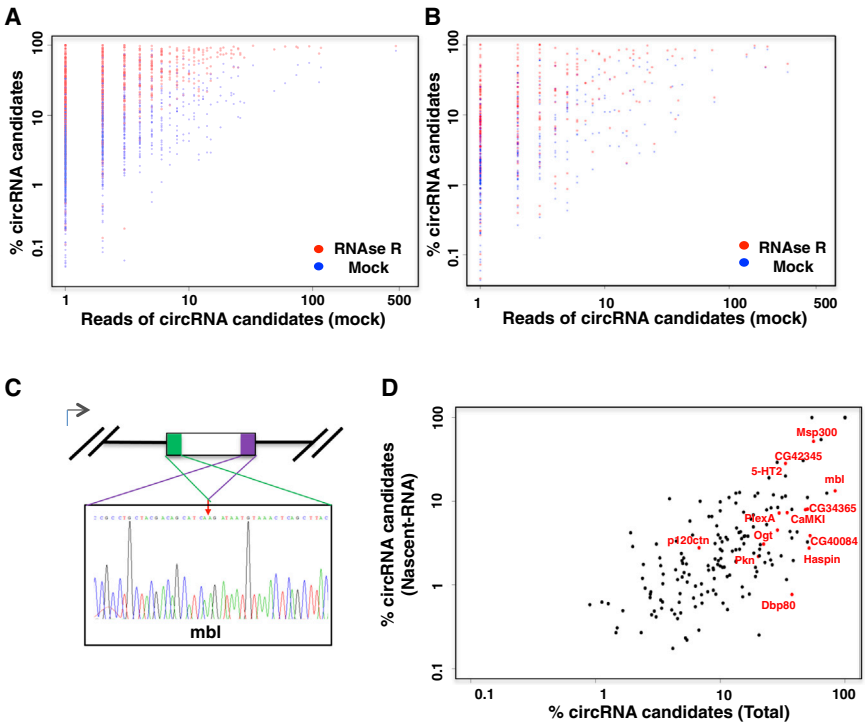

Figure 1. circRNAs Are Produced Cotranscriptionally, and Their Abundance Is Controlled at the Biosynthesis Level

(A) Identification of circRNA candidates in fly heads (n = 4). The y axis represents the percentage of circRNA candidate relative to a given exon junction.

(B) Identification of circRNA candidates in *Drosophila* S2 cells (n = 1). The y axis represents the percentage of circRNA candidate relative to a given exon junction.

(C) Validation of the circRNA hosted in the second exon of the *muscleblind* (*mbl*) gene. Sanger sequencing of a PCR product resulting from divergent primers demonstrates the head-to-tail splicing of this exon.

(D) Chromatin-bound RNA contains head-to-tail reads, and the amounts correlate with the total amount of circRNA candidates in fly heads. The x and y axes represent the percentage of circRNAs for a given junction in total or chromatin-bound RNA preparations.

Here we provide evidence that circRNAs are generated cotranscriptionally and that their production rate is mainly determined by their flanking introns. In addition, we demonstrate that canonical pre-mRNA splicing can compete with circularization of exons. Mechanisms of this competition are tissue specific and conserved from flies to humans. Strikingly, we observed that the second exon (which contains the start codon of the main coding sequence) of the splicing factor *muscleblind* (MBL/MBNL1) is circularized in both flies and humans. The introns flanking this circRNA as well as the circRNA itself contain highly conserved *muscleblind* binding motifs, and we show that MBL strongly and specifically binds to the circRNA generated from its own RNA. Furthermore, exogenous expression of *Drosophila* MBL stimulates circRNA production from endogenous fly and human *muscleblind* transcripts. The capacity of MBL to increase circMbl production is dependent on the presence of functional MBL binding sites in the flanking intronic sequences. However, sequences in both introns are necessary suggesting that MBL induces circularization by bridging between the two flanking introns. Finally, downregulation of MBL in both cell culture and fly neural tissue leads to a strong and significant decrease in circMbl production. Together, our data suggest that circRNAs have a conserved function in gene regulation by competing with canonical splicing. Moreover, we identified *muscleblind* as a regulatory factor that can promote circRNA biogenesis.

RESULTS

Cotranscriptional Production of circRNAs

Inspecting our own data (Memczak et al., 2013), we noticed that many circRNAs are generated from transcripts expressed in neuronal cells. Therefore, we measured *Drosophila* head circRNA abundance by generating and analyzing sequencing data from libraries prepared from rRNA-depleted RNA from fly heads by using our previously published computational method (Memczak et al., 2013; http://www.circbase.org; Glažar et al., 2014). In agreement with a previous report (Salzman et al., 2013), we found thousands of circRNA candidates expressed in fly heads (Figure 1A, blue dots; Table S1 available online). We also pretreated the RNA with RNase-R after rRNA depletion to make sure that sequencing reads are due to bona fide circRNAs. After RNase-R treatment, most of the identified circRNAs (2,615 out of 3,117) were highly enriched in comparison with linear mRNA isoforms (Figure 1A, compare blue and red dots). Interestingly, genes that encode neuronal proteins, with special enrichment for synaptic factors (e.g., Pkn, 5-HT2, CamKI, and many others; Figures S1A–S1C) host a highly significant number of circRNAs. To complement these data, we performed a similar experiment in *Drosophila* S2 cells. We found hundreds of circRNA candidates in this cell type as well (Figure 1B; Figure S1D; Table S1). Similarly, we also identified circRNA candidates from fly heads using an independent RNA sequencing (RNA-seq) library preparation method in which RNA fragmentation and linker ligations are done prior to reverse transcription (Figure S1B and Table S2). We confirmed the circular junctions of some of the circRNAs found in fly heads and S2 cells by quantitative RT-PCR (qRT-PCR) followed by Sanger sequencing (Figure 1C and data not shown).

To study if circRNAs are generated cotranscriptionally, we searched for circRNA reads in published data sets of chromatin-bound (nascent) RNA from fly heads (Rodriguez et al., 2013). We identified hundreds of head-to-tail junction reads in these data sets, strongly suggesting that circRNAs are generated cotranscriptionally (Figure 1D; Figure S1A; Table S3). The presence of circRNAs in these samples is unlikely to be due to

contamination with nucleoplasmic or cytoplasmic RNA as Khodor et al. (2011) showed that they contain primarily nascent RNA. The abundance of circRNAs associated with chromatin is lower than in the total RNA sample, likely due both to high stability of cirRNAs and the quick release of these molecules from chromatin after maturation. Indeed, the level of chromatin association of circRNAs is comparable to the one observed for the 3′ ends of long genes (data not shown). In addition, we found a significant correlation between the chromatin-bound and the total number of reads falling on head-to-tail junctions (Figure 1D; $r = 0.697$, $p < 0.00001$), suggesting that circRNA abundance is controlled at the biosynthesis level. We also observed circRNAs associated to chromatin in mouse liver, suggesting that circRNAs are cotranscriptionally generated also in mammals (Table S4).

Sequences that Control Exon Circularization

To study circRNA biogenesis, we used minigenes in *Drosophila* S2 and human HEK293 cells. In *Drosophila* S2 cells we focused on one highly abundant circRNA (circLuna; Figure S1D; Table S1) and two lowly expressed circRNAs: circMbl and circZfh1. These circRNAs are generated from the second exon of the gene *Luna*, the second exon of *muscleblind* (*mbl*), and the second and third exons of the gene *zfh1*. First, we determined the relative levels of pre-, mature, and circRNAs from the circRNA-forming exons in *Luna*, *mbl*, and *zfh1* by quantitative-scaled RT-PCR (see standard calibration curves in Table S5). In agreement with the RNA-seq data, *Luna* produces circRNAs with high efficiency, while *mbl* and *zfh1* generate much smaller fractions of circRNAs (Figures 2A and 2B).

We generated minigene constructs that express transcripts containing the circRNA exons and flanking intronic sequences (see Figure 2A). The only canonical 5′ or 3′ splice sites present in these minigenes are the ones flanking the ''circularizable'' exon. We generated constructs for circLuna, circZfh1, and circMbl and for an exon that is not circularized in any of our data sets: the 15th exon of the gene *timeless* (*tim*, CG3234-RA). The relative level of circularization of the RNA produced by the minigenes in *Drosophila* S2 cells strongly resembles the one observed for the endogenous genes: the Luna minigene generates more circRNA molecules than the Zfh1 or Mbl minigenes (Figure 2B). Moreover, we observed that circRNAs account for less than 45% of the RNA molecules generated from the Tim construct, demonstrating that exon circularization is not the default pathway for this type of minigene. To determine whether the high levels of the circRNAs generated from the minigenes are due to the production rate and/or stability, we cotransfected the minigenes into *Drosophila* S2 cells and followed in time the accumulation of pre- and circRNA forms generated from them. Transcription in all these minigenes is under the control of the metallothionein (MT) promoter, which is copper inducible (Bunch et al., 1988). We observed very high levels of circRNA isoforms for *Luna* after only 3 hr of transcriptional induction (Figure S2A). Interestingly, we found that the levels of circRNAs from the pMT-Tim minigene are very low few hours after induction (e.g., less than 10% of total RNA molecules at 24 hr, see Figure 2C), demonstrating that this construct generates very few (although stable) circRNAs.

We utilize a similar approach in HEK293 cells. Briefly, we generated minigenes carrying the circRNA-forming exons of the PVT1 or CRKL genes and flanking intronic sequences (Figure 2A). We also built a minigene carrying the exon 25 of EGFR, which has not been found to circularize in any system. As in *Drosophila,* circularization is more efficient for these minigenes than for the endogenous loci (Figure 2D; e.g., compare PVT1 with pcDNA-PVT1). Moreover, the EGFR exon was hardly circularized as in the context of the endogenous locus (Figure 2D).

To uncover the sequences that dictate circRNA biogenesis, we generated a new set of constructs in which we trimmed the intronic sequences in the circLuna and circMbl minigenes (Figures 2E and 2F). For the circLuna constructs, we found no difference in the circ- to pre-mRNA ratio between the minigenes carrying 1,200 or 600 bases of flanking introns and only a small decrease after reducing the length of these introns to 300 bases (Luna-300 construct; Figure 2E). However, minigenes carrying one hundred bases of the flanking *Luna* introns fail to produce almost any circRNA (Figure 2E). This is not due to deletion of consensus splicing sequences as this construct conserves both splice sites as well as a putative branching point. Moreover, introduction of an additional 500 bases of the downstream (but not upstream) intron triggered a strong increase of the circRNA levels (Figure 2E). Interestingly, this is not due to specific sequences present in the *Luna* intron, as introduction of 500 bases from the *tim* intron also rescues the circularization defects observed in the minigene carrying 100 bases of flanking introns.

Similar experiments performed with the *mbl* minigene also suggest a key role for flanking intronic sequences in regulation of exon circularization. The *mbl* minigene generates approximately 60% of circRNA molecules (Figures 2B and 2F). While truncation of 130 bases from the flanking introns does not affect circularization efficiency, further truncation of the intronic sequences (mbl-300 construct) results in a strong decrease in the amount of circRNAs produced from the minigene (see Figure 2F, bottom panel). Intriguingly, additional deletion in the flanking introns results in increase in the levels of circRNAs. To explain these results, we searched for complementary sequences between the two flanking introns present in the *mbl* minigene. Indeed, we found numerous reverse complementary repeats between the two flanking introns (see Figure S2B), suggesting that circRNA biogenesis in this minigene might be mediated by sequence-dependent folding of the pre-mRNA (as previously proposed for alternatively spliced exons; see Raker et al. 2009). We therefore assessed the abilities of the pre-mRNAs generated from the different *mbl* minigenes to fold into secondary structures using RNAfold (Lorenz et al., 2011). Briefly, for each nucleotide in the upstream intron we summed up the probabilities of pairing with any of the nucleotides in the downstream intron. Subsequently, the same procedure was applied to the nucleotides in the downstream intron. The results of this analysis mirror the circularization efficiencies observed with the truncated *mbl* minigenes (compare Figure 2F with Figure S2C). The flanking intronic sequences in the mbl-730, mbl-600, and mbl-100 minigenes are predicted to interact strongly (Figure S2C) and produce circRNAs efficiently (Figure 2F). The intronic sequences in the mbl-300 minigene, which generate circRNAs with lower efficiency (Figure 2F), are not predicted to interact. Together, these results point toward a key role for flanking introns in determining circularization efficiency.

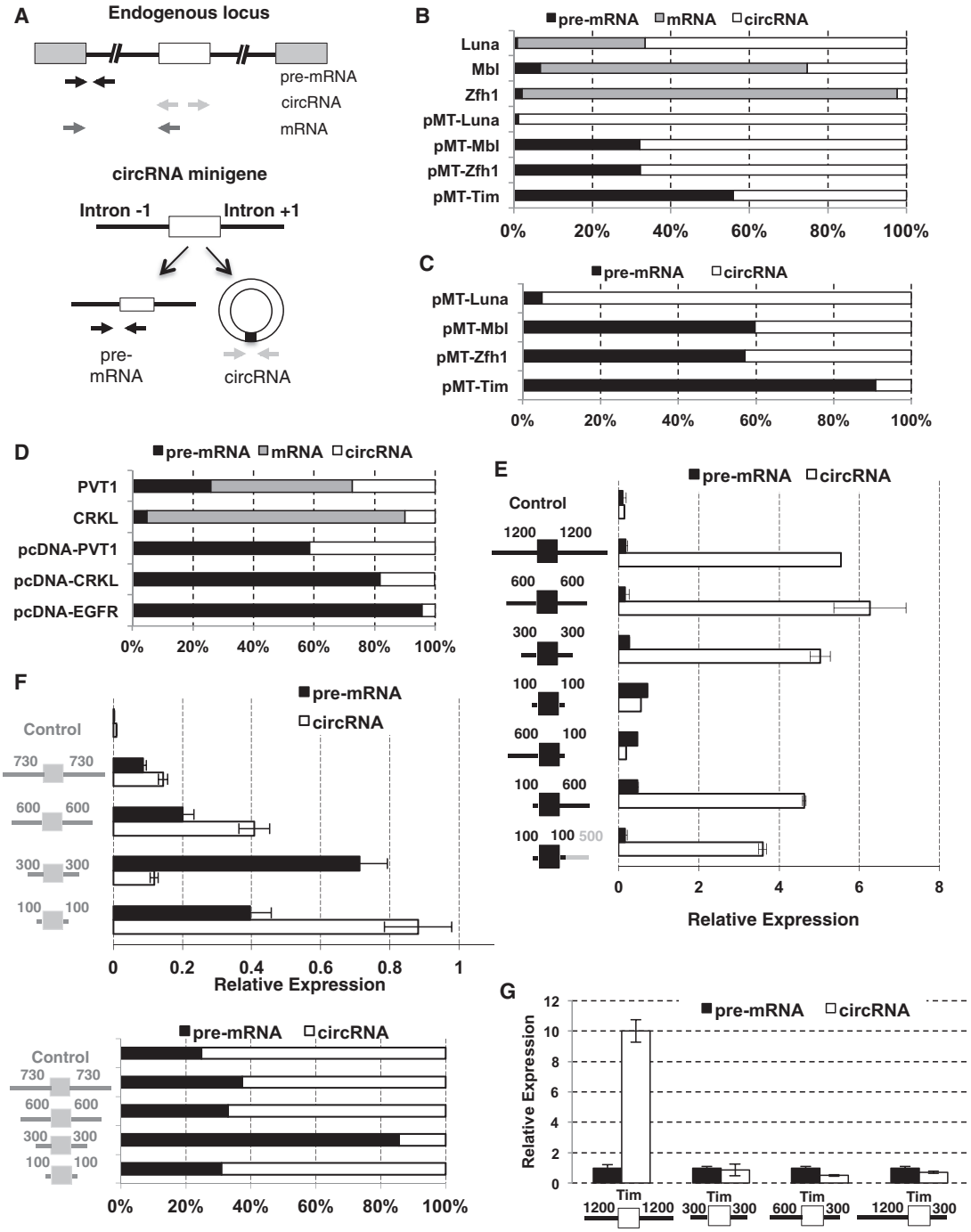

Figure 2. Sequences that Control Exon Circularization

(A) Strategy utilized for detecting endogenous or minigene-derived circRNAs.

(B) qRT-PCR measurements of the levels of pre-mRNA, circRNA, or mRNA from the endogenous or the minigene-expressed exons (n = 9). Measurements were performed 48 hr after copper stimulation.

(C) qRT-PCR measurements for pre- and circRNA from the specified minigenes at 24 hr following copper stimulation (n = 4).

(D) Levels of pre-mRNA, circRNA and mRNA for the endogenous or the minigene-expressed PVT1, CRKL, and EGFR (measured by qRT-PCR, n = 4).

(E) Sequences in the intron downstream of circLuna are necessary for efficient exon circularization (n = 4, normalized to *rp49;* mean ± SE). Black lines indicate circLuna flanking intronic sequences and gray *tim* intronic sequences.

(F) Truncation of the intronic sequences flanking circMbl suggests that they are involved in regulation of exon circularization. The upper panel represents the data normalized to *rp49* (n = 4, mean ± SE), and the bottom panel represents the percentage of both forms in each sample.

(G) Introns flanking *Luna* second exon are enough to drive circularization of *tim* exon (n = 6, normalized to *rp49*; mean ± SE).

To determine whether flanking intronic sequences are sufficient to promote efficient circularization, we generated a minigene containing the *tim* exon flanked by the introns from the circLuna minigene. Indeed, in this *tim-Luna* hybrid minigene, circularization efficiency of the *tim* exon reaches levels comparable to the *Luna* exon (Figure 2G, compare with Figure 2B). Thus, *Luna* introns are sufficient to promote efficient exon circularization.

To test whether sequences in the *Luna* exon could also have a role in exon circularization, we generated a minigene containing the control *tim* exon flanked by 300 bases of the *Luna* intron (Luna300-Tim-Luna300 construct). While the Luna-300 constructs generate mostly circLuna molecules (Figure 2E), the new construct failed to generate significant amounts of circTim (Figure 2G). These results suggest that although introduction of introns flanking circRNAs are sufficient to promote efficient exon circularization, sequences in the exon that is circularized are also important to determine the circularization rate when flanking introns are short. Interestingly, addition of longer introns (600 or 1,200 bases) upstream of the circularizable exon is not enough to promote circularization (Figure 2G, last two constructs).

To determine whether the circularization mechanisms are conserved, we tested if the Luna minigene could also produce circRNAs in human cells. Strikingly, we observed that the *Drosophila* construct generates circRNAs also in mammalian cells (HEK293; data not shown).

To explore the relationship between splicing and circRNA biogenesis, we compared the levels of circRNAs generated from *Luna* and *zfh1* with the splicing efficiency of their flanking exons in S2 cells and fly heads. We generated and sequenced stranded RNA-seq libraries from rRNA-depleted S2 cells RNA and compared sequencing results with the ones generated from fly heads. We observed that both genes, which generate circRNAs to much higher degrees in S2 cells, are less efficiently spliced in these cells than in fly heads (Figure S3A), suggesting that circRNA generation and splicing are in competition.

CircRNA Production and Pre-mRNA Splicing Compete with Each Other

To determine globally the relationship between circRNA biogenesis and canonical splicing, we measured the efficiency of cotranscriptional splicing genome-wide. We utilized the nascent-seq data sets (Rodriguez et al., 2013). We found that the splicing efficiency of the introns flanking the 50 highest expressed circRNAs is significantly lower than the splicing efficiency of all introns (Figure 3A). This is likely due to the fact that circRNAs are flanked by considerably longer introns (see Jeck et al., 2013 and Figure S3B), which are less efficiently spliced cotranscriptionally (Khodor et al., 2012).

To determine whether there is a genome-wide competition between canonical splicing and circRNA generation, we increased the efficiency of linear splicing and monitored the effect on circRNA biogenesis. If there is competition, circRNA abundance should decrease in a context where linear splicing is more efficient. To test this possibility, we used flies carrying a variant of the large subunit of the RNA polymerase II. This mutation decreases the elongation capacity of RNA pol II (C4 flies or "slow polymerase flies" [Coulter and Greenleaf, 1985]), which has been shown to increase cotranscriptional splicing efficiency both in flies and in mammals (de la Mata et al., 2003; Ip et al., 2011; Khodor et al., 2011). Briefly, we generated total and circRNA-enriched (RNase-R treated) RNA-seq libraries from the heads of flies carrying the C4 mutation and isogenic controls, and we measured the ratios of linear to circular RNAs. We found that flies with the mutation produce a significantly lower number of circRNAs, even when normalized to the linear forms of the same gene (Figure 3B). This was true for most circRNAs independently of their expression level.

The negative correlation between splicing efficiency and circRNA biogenesis rates suggests that circularization of exons is carried out by the canonical splicing machinery. To test this possibility we mutated the 5′ splice sites flanking the PVT1 or CRKL exons in our minigenes. Mutation of the 5′ splice sites from GU to CA strongly diminishes the generation of circRNAs from this minigene, demonstrating that exon circularization is spliceosome (or at least U1)-dependent (Figure 3C).

Our results suggest strong competition between circRNA biogenesis and canonical splicing. As stated above, minigenes carrying circRNA exons and flanking introns efficiently generated circRNAs (Figures 2B and 2C). Interestingly, introduction of flanking exons carrying strong 5′ and 3′ splice sites dramatically decreases the circularization efficiency of the *Drosophila* Luna minigene, demonstrating strong competition between exon circularization and canonical splicing (Figures 3D and 3E). Even the presence of just one exon downstream (Luna p-C-E construct) was enough to decrease circRNA formation more than 4-fold (Figures 3D and 3E).

To extend our observation to human cells, we introduced the flanking exons to the mammalian minigenes described above, transfected them into HEK293 cells, and determined relative levels of the mRNA, pre-mRNA, and circRNA by scaled qRT-PCR. Introduction of flanking exons strongly competed with exon circularization, again demonstrating competition between exon circularization and splicing (Figures 3D and 3E, see PVT1 and CRKL panels). Moreover, mutating the splice sites of the flanking exons in the PVT1 almost fully restores the circularization rate to the level of the construct without competition. The lack of response to these mutations in the CRKL construct is due to the presence of cryptic splice sites in the minigene that are used by the spliceosome, and competition is therefore not abolished (Figure 3F).

As shown above, introns flanking circRNAs are in general less efficiently spliced cotranscriptionally than those that do not (Figure 3A). This is likely due in part to their increased length (Figure S3B). To determine if the generation of circRNAs per se may also have an effect on the rate of canonical cotranscriptional linear splicing, we measured the splicing efficiency of chromatin-bound RNA that contain introns hosting circRNAs and of control introns with similar lengths. In all cases we found that the introns that bracket circRNAs are less efficiently spliced than other introns of similar size or position in the gene (Figures 3G and S3B). These data suggest that the decrease in linear splicing of introns flanking circularized exons is dependent on intron sequences, which promote circularization at the expense of linear splicing. Thus, circRNA production seems to have a negative effect on linear splicing and therefore on gene expression.

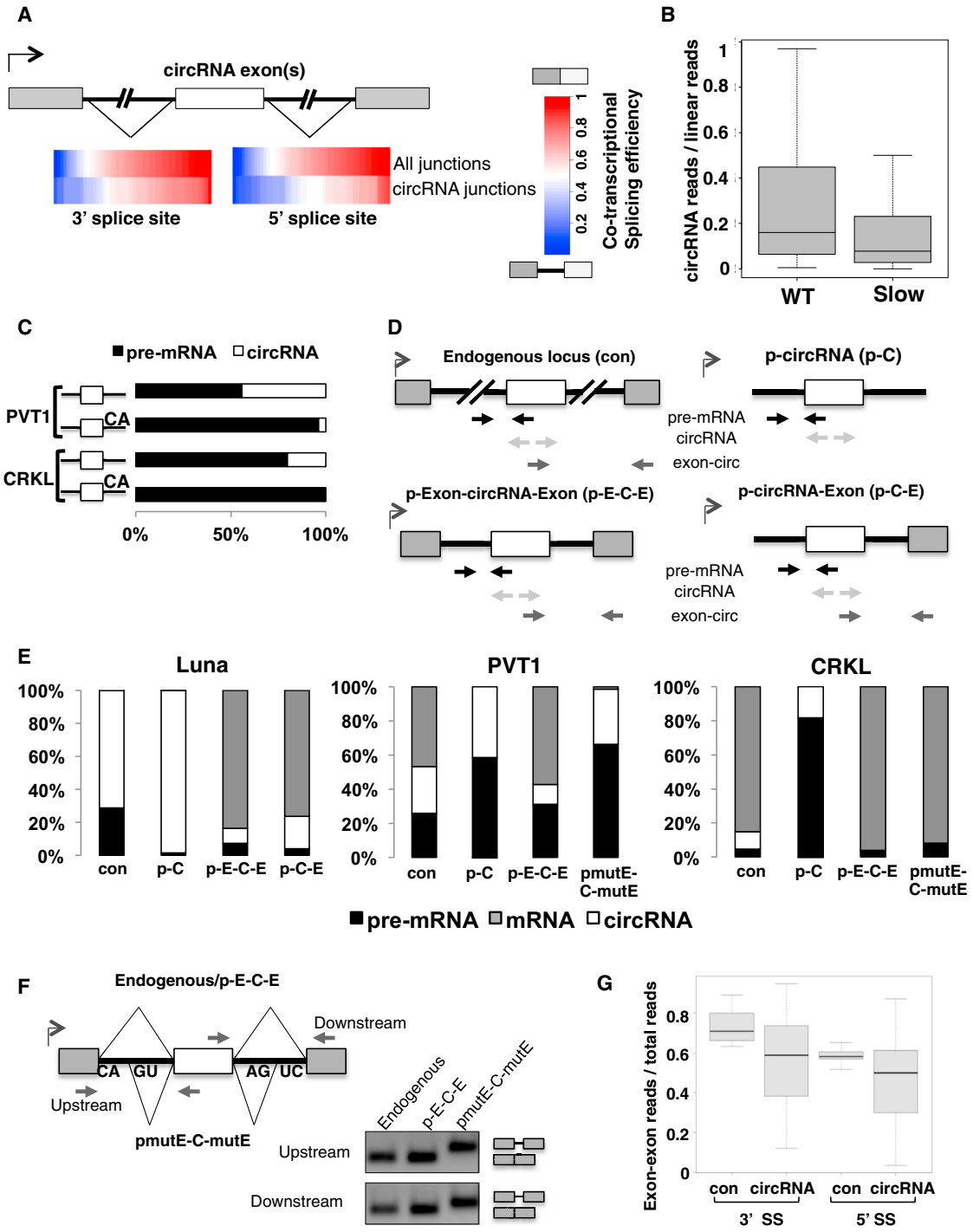

Figure 3. Competition between Canonical and Scrambled Splicing Determines the Levels of circRNAs

(A) Introns bracketing circRNAs are less efficiently cotranscriptionally spliced than control introns. The splicing efficiency was calculated from chromatin-bound RNA for each 5′ or 3′ splice site as mRNA reads/(mRNA reads + pre-mRNA reads + circRNA reads). The control group represents the distribution of splicing efficiency for all junctions in the fly genome. Mann-Whitney U-test demonstrated significant difference between the groups ($p < 0.0001$).

(B) C4 (slow polymerase) flies have a significant lower number of circRNAs. The count of circRNA reads is normalized to the linear forms of the same junction. Data are presented as a box-and-whisker plot ($p < 0.0001$, Mann-Whitney U-test).

(C) Disruptive mutations of the circRNA exon splice site by a GU to CA mutation strongly diminish the generation of circRNAs from the minigene (n = 3).

(D) Scheme of the minigenes containing 5′ and/or 3′ competing exons.

(E) Introduction of flanking exons carrying strong 5′ and 3′ splice sites dramatically decrease the circularization efficiency of the minigenes, but mutating these splice sites (GU to CA and AG to UC) abolishes competition for the PVT1 construct (measured by qRT-PCR, n = 4).

(legend continued on next page)

muscleblind Can Regulate circRNA Production

Intriguingly, the most abundant circRNA in fly heads originates from the second exon of the gene *muscleblind* (*mbl*/*MBNL1*; Figures 1C and 1D; Figure S1A; Table S1), a well-characterized splicing factor (Wang et al., 2012). In fly heads, this circRNA (Houseley et al., 2006) is more abundant than the canonical, protein-coding mRNA (Figure S1A), but circMbl is present at much lower levels in *Drosophila* S2 cells (Figure 2B; Table S1). At the same time, *Drosophila* S2 cells lack the MBL protein isoform predominantly expressed in fly heads (Figure 4A and Figure S4A, first two lanes).

Interestingly, we discovered many putative MBL binding sites in the intronic sequences flanking the second exon of *mbl* (Figure 4B). The presence of these binding sites suggests that some of the MBL isoforms (i.e., the form present in fly heads) might promote the production of circRNA from its own exon. To test this possibility, we transfected S2 cells with plasmids driving the expression of three different MBL variants. Among them was MBL-C, the predominant MBL isoform in fly heads (Figures 4A and S4A) and MBL-A, also a short isoform of *muscleblind*, which may function similarly to MBL-C based on their analogous structure. The expression of MBL-A and MBL-C each lead to a 3-fold increase in circMbl expressed from the endogenous locus (Figure S4B). As transfection efficiency is less than 30%, we repeated the experiments after purifying transfected cells by fluorescence-activated cell sorting (FACS). Indeed, in this cell population, we observed a 13-fold increase in circMbl levels following expression of MBL-A or MBL-C (Figure 4C). The effect is specific, as the levels of two other circRNAs, circFoxo, and circPKN are not affected by MBL overexpression (Figure 4C). Interestingly, the levels of a second circRNA, circLuna were increased 3-fold. This may be explained by the presence of 17 putative binding sites (4-mer sites) for MBL in the *Luna* introns and circRNA (Figure S4C). The strong effect of MBL-A and MBL-C on the levels of circMbl is accompanied by a 2-fold decrease in the levels of the endogenous *mbl* mRNA. Given the relative levels of circMbl and mRNA in S2 cells prior to MBL transfection, the 13-fold increase in circMbl correlates well with the 2-fold drop in linear *mbl*. In light of our previous results about competition between circRNA biogenesis and splicing, we infer that MBL promotes circularization of its own exon 2 to the detriment of mRNA production.

MBL-A overexpression leads to a strong increase of circMbl production also from the pMT-Mbl minigene even in the presence of low amounts of MBL-expressing plasmid (Figure 4D). The effect of MBL overexpression on the pMT-Mbl minigene is specific, as we did not observe an increase of circTim levels from the pMT-Tim minigene upon MBL overexpression (Figure 4D, right).

Strikingly, we noticed that the same exon of human MBNL1 (the mammalian homolog of *mbl*), as well as the second exon of mouse MBNL2, also generates putative circRNAs (Glažar et al., 2014). The human MBNL1 exon and its flanking introns also contain abundant putative *mbl* binding sites, which lie in regions of very high evolutionary conservation (Figures S5A and S5B). Moreover, utilizing previously published CLIP-seq (cross-linking and immunoprecipitation followed by high-throughput RNA-sequencing) data, we found that the murine homolog of MBNL1 strongly binds to the same exon as well as to the second exon of MBNL2 (Figure S5C). To determine whether the role of *muscleblind* in circRNA biogenesis is conserved in mammals, we transfected the *Drosophila* MBL isoforms into HEK293 cells and measured the expression levels of the circRNA generated by the endogenous *MBNL1* locus. Indeed, we observed a consistent increase in the levels of the circRNA of this exon upon expression of MBL-A and MBL-C, demonstrating the conserved role for *muscleblind* in exon circularization (Figure S5D).

As MBL is also involved in mRNA localization and stability, it is possible that the observed effects of this protein on circRNA production are due to regulation of circRNA stability rather than biosynthesis. Therefore, we determined the stability of the different *mbl* RNA species (mRNA, pre-mRNA, and circRNA) in S2 cells (control) and in cells stably transfected with the MBL-A plasmid upon arrest of transcription. Incubation of the cells with Actinomycin D leads to a quick decrease in the levels of an unstable mRNA, the one encoding the circadian protein *cycle* (Figure 4E). As previously reported for other circRNAs (Jeck et al., 2013; Memczak et al., 2013), circMbl is unusually stable and its level did not decrease in the assayed time frame. Importantly, we did not detect differences between the control cells and the cell line overexpressing MBL (Figure 4E). Moreover, we did not observe any significant effect of MBL overexpression on the decay rates of either *mbl* mRNA or pre-mRNA. To complement these data, we measured the decay rate of *mbl* pre- and circRNAs generated from the *mbl* minigenes in the absence or presence of MBL overexpression. We cotransfected S2 cells with either the *mbl* minigene and a control or an MBL-expressing plasmid, induced transcription with copper for 12 hr, and assessed the levels of circMbl and *mbl* pre-mRNA from samples collected at different time points following incubation of the cells in media without inducer. We did not observe any clear effect of MBL overexpression in the stability of *mbl* pre- or circRNA species (data not shown).

Requirements for MBL-Induced Circularization

To gain insights into the mechanism by which MBL induces circMbl formation, we tested the effect of MBL overexpression on the mbl-100, -300, and -600 minigenes. The circularization efficiency achieved in the presence of MBL overexpression is highly dependent on the length of the *mbl* flanking intronic sequences and more specifically on the number of putative MBL binding sites (Figures 5A and 4B). While there are 25 predicted MBL

(F) Cryptic splice sites in the introns are used in the transcript expressed from the CRKL minigene. Longer PCR amplicons are produced from the mutated mRNAs using upstream or downstream exons primers. Sanger sequencing of these amplicons reveals that a GU 45 nucleotides downstream of the mutated splice site and an AG 34 nucleotides upstream of the mutated 3′ splice site are used.

(G) Exons harboring circRNAs display lower cotranscriptional splicing efficiency than exons of the same length. Splicing efficiency was calculated from chromatin-bound RNA-seq data. Data are presented as a box-and-whisker plot. The Mann-Whitney U-test and sampling approach (1,000 samples) showed significant difference between the groups ($p < 0.0005$ and $p < 0.05$, respectively).

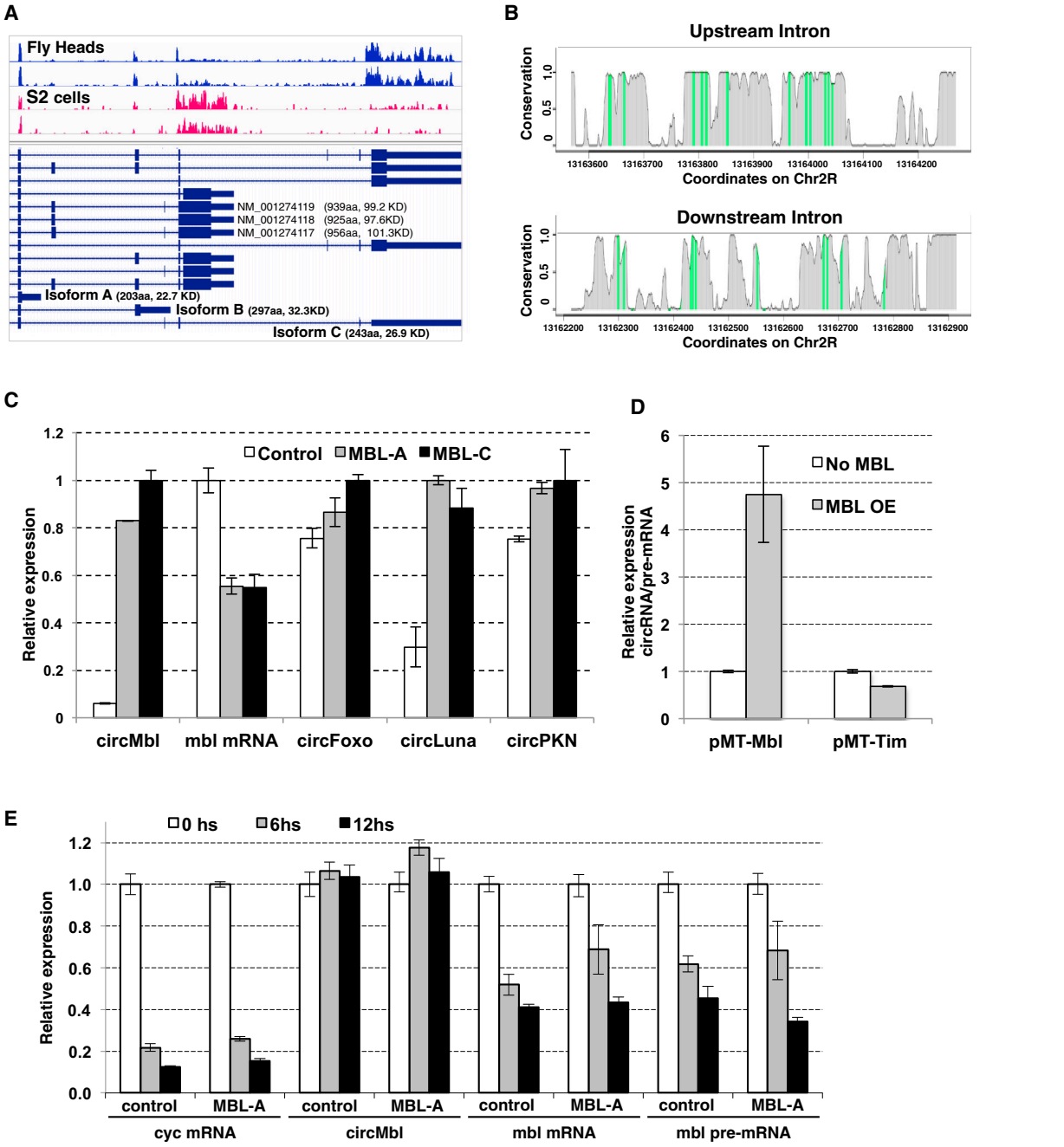

Figure 4. *muscleblind* Can Promote Exon Circularization

(A) *Drosophila* S2 cells express alternative mRNA isoforms of *mbl*. For easier visualization, only the 3′ end of the *mbl* gene is displayed.

(B) Predicted MBL binding sites in the sequences flanking the second exon of *Drosophila mbl*. Green lines indicate MBL putative binding sites, and the heights indicate evolutionary conservation.

(C) Expression of MBL-A and MBL-C promote the formation of circMbl and circLuna. *Drosophila* S2 cells were cotransfected with a plasmid encoding an MBL isoform or empty plasmid and a GFP-expressing plasmid. Transfected cells were purified by FACS sorting (n = 6, mean ± SE). Expression levels were measured by qRT-PCR and normalized to *rp49*.

(D) MBL expression increases circularization efficiency from the circMbl, but not from the circTim minigene. MBL OE refers to cotransfection of 0.25μg of an MBL-A expressing plasmid with the minigenes (n = 15, mean ± SE).

(E) MBL overexpression does not change the decay rates of either circMbl, *mbl* mRNA, or pre-mRNA. Transcription arrest was induced by treating S2 cells overexpressing MBL-A protein (stable line) and control S2 cells with 1μg/ml Actinomycin D for the indicated times. Expression was normalized to *rp49* (n = 3, mean ± SE).

binding sites in the circMbl flanking introns in the mbl-730 construct, there are 24 sites in the mbl-600 construct, 10 in the mbl-300, and only 2 in the mbl-100 minigene. Strikingly, all constructs but mbl-100 produce circMbl with higher efficiency following MBL overexpression, even mbl-300, which before generated low levels of circRNAs (likely due to the lack of base pairing between the flanking introns; Figures 2F and S2C). The lack of response by mbl-100 to MBL overexpression is likely due to the fact that it has only two MBL binding sites in the flaking introns. Together these data suggest a direct effect of MBL on circMbl biosynthesis.

In addition to the putative MBL binding sites present in the flanking introns, the *mbl* exon 2 itself is significantly enriched in predicted MBL binding sites. These sites are well conserved among *Drosophila* species and are also present in mouse and humans (see Figure S5A). Thus, MBL may bind directly to its own exon and thereby regulate its circularization. To test this possibility, we utilized the stable line expressing MBL-A protein and performed an RNA immunoprecipitation (RIP). circMbl was strongly associated with MBL, unlike other tested circRNAs and mRNAs (Figure 5B).

To unequivocally establish the importance of the exonic and intronic putative MBL binding sites, we generated plasmids containing disruptive mutations (GC to CA as in Goers et al., 2010) in all the flanking intronic or exonic MBL binding sites. Mutation in the exonic binding sites affected only partially the ability of MBL to increase circMbl biogenesis (Figure 5C, center, Mbl-Mut-Mbl). However, mutation of the putative MBL binding sites in the introns abrogates most of the effect of MBL on circMbl biogenesis (Figure 5C, right, Mut-Mbl-Mut construct).

To determine whether the *mbl* intronic sequences alone are sufficient to mediate mbl dependence, we generated a new set of constructs carrying the TIM exon flanked by *mbl* introns in their wild-type or mutated versions. Overexpression of MBL leads to a more than 2-fold increase of circTim production when it is flanked by *mbl* introns, whereas it does not affect (or even decreases) the relative levels of circTim that arises from the pMT-Tim construct (Figure 5D). Conversely, a minigene in which the MBL exon is flanked by the tim intronic sequences is insensitive to MBL overexpression. These experiments demonstrate that the flanking circMbl intronic sequences can confer MBL-dependent circularization. Thus, MBL regulation is mostly achieved through binding to the flanking introns of the circRNA (Figure 5D, center). In addition, mutations of the MBL sites in the flanking *mbl* introns of the mbl-Tim-mbl minigene abrogate most of the effect observed upon MBL overexpression (Figure 5E). Interestingly, mutation of the MBL sites in only one of the flanking introns is sufficient to significantly hinder the effect of MBL on circularization (Figure 5E). This suggests that efficient MBL-induced circularization depends more on the binding of MBL to both introns simultaneously than on the total number of MBL binding sites (e.g., the mbl-300 minigene has 10 and the Mut-Tim-Mbl and Mbl-Tim-Mut minigenes have 12 and 13 binding sites respectively; the effect of MBL on the mbl-300 minigene is much stronger, compare Figure 5A with Figure 5E).

To test whether MBL binds the Mbl-Tim-Mbl pre-mRNA and if mutating the MBL binding sites in the flanking introns abrogates this association, we performed RIP against a myc-tagged MBL protein from cells transfected either with a Mbl-Tim-Mbl or a Mut-Tim-Mut minigene. While the Mbl-Tim-Mbl pre-mRNA was strongly associated with MBL (Figure 5F), mutation in the putative binding sites significantly diminished this association. Importantly, we found a similar enrichment for circMbl in both immunoprecipitates, demonstrating equal efficiencies in both immunoprecipitations.

If MBL is a circRNA-promoting factor, knockdown of MBL should decrease the levels of this circRNA. Indeed, knockdown of endogenous *mbl* in S2 cells by the use of *mbl* double-stranded RNA (dsRNA) leads to a 2-fold decrease in the levels of circMbl, but not circPkn (Figure 5G and data not shown). Importantly, the dsRNA targets the first exon of *mbl* and does not include any sequence present in the circRNA. Moreover, the lower levels of circMbl are not due to changes in transcription, as *mbl* pre-mRNA levels were not affected in this experiment (Figure 5G).

As circMbl is highly abundant in fly heads, we decided to study the effect of knocking down MBL in neural tissues by expressing an RNAi hairpin against *mbl* under the control of the pan-neuronal GAL4 driver *elav*. The construct used is directed against the first exon of *mbl* and does not target the second exon that generates the circRNA. In agreement with our previous results, we observed a strong decrease (almost 6-fold, Figure 5H) in the levels of circMbl. The results shown in Figure 4C demonstrate that MBL can promote the formation of circMbl and circLuna. As circLuna is very lowly expressed in fly heads we searched for circRNAs that are present at high levels in fly heads and are flanked by putative MBL binding sites (see Experimental Procedures). We checked the levels of two of these candidates (circHaspin and circPk61C) upon mbl knockdown. In agreement with a more general role of MBL in circRNA biogenesis, we observed a strong decrease (3-fold) in circHaspin upon knockdown of *mbl* in fly neural tissue.

DISCUSSION

Here we present a comprehensive study of circRNA biogenesis. Our data strongly suggest that circRNAs are processed cotranscriptionally. As mutating splice sites immediately flanking circularized exons abolishes circularization, our data provide evidence that circRNAs are generally produced by the spliceosome. The spliceosome is further implicated in circRNA production since circularization rates were strongly dependent on the presence of canonical splice sites of bracketing exons. Thus, linear splicing of flanking exons can compete with circRNA biogenesis. We note that these competition effects are strong and can reduce circRNA levels by an order of magnitude.

We show that flanking intronic sequences are the main factor that determines circularization efficiency of a given exon. Genes harboring circRNAs are less efficiently spliced compared with control genes of similar intron length. Thus, intronic sequences that promote circularization appear to be responsible for a reduction in linear splicing efficiency of flanking exons. Since we have shown that splicing is directly involved in forming circRNAs, we conclude that circRNA production likely modulates linear splicing. Together, our data suggest that linear splicing and circRNA production mutually regulate each other by

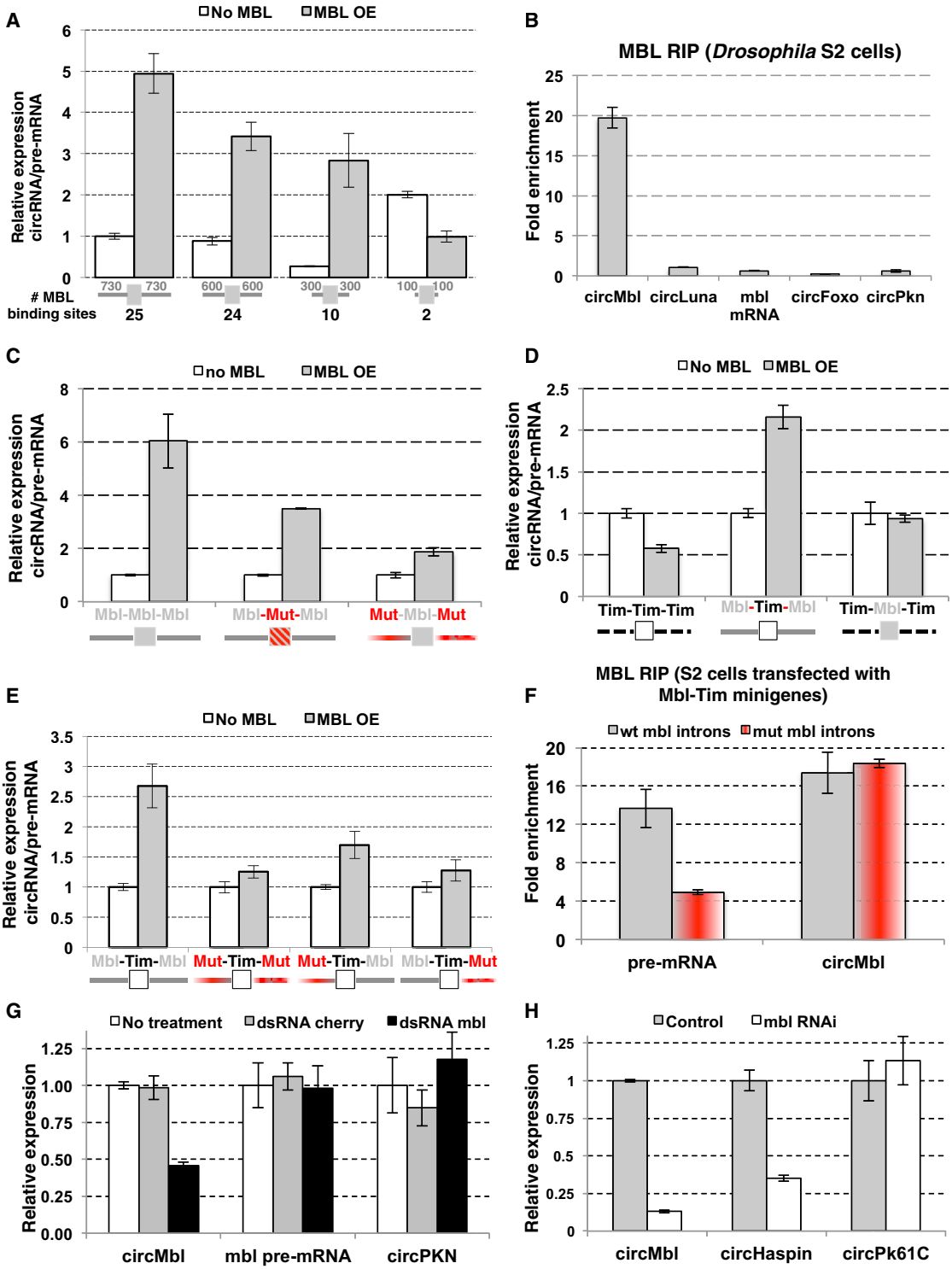

Figure 5. *muscleblind* Directly Interacts with circMbl and Its Flanking Introns and Promotes Exon Circularization

(A) MBL dependence is inversely proportional to the length of the *mbl* flanking intronic sequences (n = 4, mean ± SE). The numbers below the schemes indicate the number of MBL binding sites in the flanking introns of each construct.

(B) circMbl is strongly associated with MBL. RNA immunoprecipitation for myc-tagged MBL from *Drosophila* S2 cells (in MBL-A stable line). The fold-enrichment was calculated as a ratio between the IP and INPUT fractions for the specific target and a control RNA (*vri*). Mean ± SE (n = 6).

(C) Mutation of the putative MBL binding sites of circMbl flanking introns abrogates most of the effect of MBL on circMbl biogenesis (n = 6, mean ± SE). Gray lines or boxes represent the wild-type sequences of *mbl* introns and exon, respectively. Red lines and boxes represent mutated sequences.

(legend continued on next page)

competing for splice sites. In fact, it is entirely possible that the main regulatory impact of most circRNAs is on linear splicing of the host mRNA. Indeed, increasing the efficiency of canonical splicing by diminishing the elongation capacity of RNA polymerase II (C4 flies) leads to a decrease in the levels of circRNAs. In addition, our experiments suggest that exonic sequences are also important in the context of short flanking introns. Lastly, we found a factor that can promote circRNA biogenesis, the splicing factor *muscleblind.* We show that modulation of *mbl* levels affects the production rate of at least three circRNAs. Our data support a direct role for MBL in circMbl biosynthesis. The introns flanking circMbl have many MBL binding sites, which are essential to make circularization rates of bracketed exons dependent on MBL levels. Moreover, we found a strong and direct interaction between this protein and circMbl. This raises the possibility of a sophisticated control mechanism for MBL levels. When the protein is in excess, it decreases the production of its own mRNA by promoting circMbl production. This circRNA could then sponge out the excess MBL protein by binding to it.

Our results suggest that general splicing factors may determine the balance between circRNA biogenesis and canonical splicing. They could do so by inhibiting or enhancing the splicing of the introns upstream of the "circularizable" exons. Importantly, the conserved role of *mbl* in exon circularization and the capacity of mammalian cells to circularize a *Drosophila* exon demonstrate that mechanisms of circRNA biogenesis are conserved between these organisms. This is surprising because of the differences in splicing mechanisms between flies and mammals: exon definition is dominant in humans and mouse, whereas intron definition predominates in *Drosophila* (Khodor et al., 2012). Finally, the fact that circRNA host transcripts are significantly enriched in neural-related genes provides a link between RNA binding proteins and brain function and/or maintenance. Indeed, alterations in the level and/or function of RNA-binding proteins like TDP-43, Ataxin-1, and *muscleblind* cause well-studied neurodegenerative disorders (Buratti and Baralle, 2011; Osborne and Thornton, 2006; Yue et al., 2001). This suggests that abnormal circRNA biogenesis may have a role in these diseases or that circRNAs could be used for biomarking these disorders. In support of this idea, reduced levels of CDR1as/ciRS-7 circRNA have already been reported in patients suffering from Alzheimer's disease (Lukiw, 2013).

EXPERIMENTAL PROCEDURES

Detection of circRNAs by RNA-Seq and qRT-PCR

RNA was extracted using TRI Reagent (Sigma). Depletion of rRNA was performed using Ribominus kit (Invitrogen). RNase-R treatments were performed by adding 3U of RNase-R (Epicenter Biotechnologies) per μg RNA and 15 min incubation at 37°C. cDNA libraries were generated using the TruSeq RNA sample preparation kit and protocol (Illumina), and stranded, ligation-based libraries were performed as previously described (Engreitz et al., 2013).

Cell Culture Experiments

Drosophila S2 cells and HEK293 cells were cultured using standard protocols. Transfections were performed using Mirus TransIT2020 (S2 cells) or Lipofectamine 2000 (HEK293).

RNA Immunoprecipitation

The protocol is based on Kadener et al. (2009).

Computational Analysis of circRNAs and Splicing Efficiency

circRNA detection in RNA-seq data was performed as previously described (Memczak et al., 2013). *Drosophila* and mouse nascent RNA-seq data were obtained from the Gene Expression Omnibus database (GEO) (under accession numbers GSE32950 and GSE36916, respectively). Comparison of circRNAs between wild-type and slow polymerase flies was done by counting the reads aligned to the circRNA junctions and normalizing to the number of reads from the linear exon-exon junctions at the same position.

Identification of circRNAs Enriched for Putative MBL Binding Sites

circRNAs were scanned for enrichment of the following 4-mer motifs: 5′-CGCT-3′, 5′-TTGC-3′, 5′-CTGC-3′, 5′-TGCT-3′, and 5′-GCTT-3′. The p values were calculated as the fraction of permutation values that are at least as extreme as in circRNA itself.

ACCESSION NUMBERS

All raw sequencing data are available for download from the National Center for Biotechnology Information GEO database under accession number GSE55872.

SUPPLEMENTAL INFORMATION

Supplemental Information includes Supplemental Experimental Procedures, five figures, and five tables and can be found with this article online at http://dx.doi.org/10.1016/j.molcel.2014.08.019.

AUTHOR CONTRIBUTIONS

R.A.-F, M.H., and S.M. generated and analyzed the RNA-seq data. M.M. performed the HEK293 experiments. N.R.P., R.A.-F., M.H, N.E., and O.B. performed the *Drosophila* S2 cell and the fly head experiments. A.I. performed the analysis of MBL/MBNL1 binding sites. N.R. and S.K. designed and supervised the project.

ACKNOWLEDGMENTS

We thank Prof. Monckton and Prof. Artero for reagents. We thank Prof. G. Ast and Prof. A. Kornblihtt for useful discussions. We acknowledge the following funding sources: the International Human Frontiers Science Program Organization (CDA no. 10/2009 to S.K.), the European Research Council Starting Grant (ERC no. 260911 to S.K.), and the Israeli Science Foundation Personal Grant (no. 1015/10 to S.K.). A.I. is funded by the German-Israeli Foundation (GIF). S.M. was funded in part by the Federal Ministry of Education and Research

(D) circMbl flanking introns are sufficient to make circTim formation sensitive to MBL levels (n = 9, mean ± SE).
(E) Mutations of the MBL sites in the flanking *mbl* introns of the mbl-Tim-mbl minigene abrogate most of the MBL dependence (n = 6, mean ± SE).
(F) Mutation of putative MBL binding sites of circMbl flanking introns decreases MBL binding to the pre-mRNA. *Drosophila* S2 cells were transfected with minigenes containing circTim exon flanked by *mbl* introns with or without mutation of MBL binding sites. Fold-enrichment was calculated as the ratio between the IP and INPUT fractions (n = 6, mean ± SE). circMbl levels were used as a control to demonstrate similar IP efficiency between samples.
(G) Expression of circMbl, *mbl* pre-mRNA, and circPkn from control or *mbl* dsRNA treated *Drosophila* S2 cells. Expression was normalized to *rp49* (n = 3, mean ± SE).
(H) Expression of circMbl, circHaspin, and circPk61C from control (*elav-gal4*) and *mbl* RNAi (elav-gal4;UAS-mblRNAi/UAS-*Dcr2*) flies. Expression was normalized to *rp49*, mean ± SE, n = 3.

(BMBF, no. 01KU1216D, DEEP) and by the German Research Foundation (DFG, no. RA-838/7-1).

Received: July 11, 2014
Revised: August 11, 2014
Accepted: August 14, 2014
Published: September 18, 2014

REFERENCES

Bentley, D.L. (2014). Coupling mRNA processing with transcription in time and space. Nat. Rev. Genet. *15*, 163–175.

Braun, S., Domdey, H., and Wiebauer, K. (1996). Inverse splicing of a discontinuous pre-mRNA intron generates a circular exon in a HeLa cell nuclear extract. Nucleic Acids Res. *24*, 4152–4157.

Bunch, T.A., Grinblat, Y., and Goldstein, L.S.B. (1988). Characterization and use of the *Drosophila* metallothionein promoter in cultured *Drosophila melanogaster* cells. Nucleic Acids Res. *16*, 1043–1061.

Buratti, E., and Baralle, F.E. (2011). TDP-43: new aspects of autoregulation mechanisms in RNA binding proteins and their connection with human disease. FEBS J. *278*, 3530–3538.

Capel, B., Swain, A., Nicolis, S., Hacker, A., Walter, M., Koopman, P., Goodfellow, P., and Lovell-Badge, R. (1993). Circular transcripts of the testis-determining gene *Sry* in adult mouse testis. Cell *73*, 1019–1030.

Coulter, D.E., and Greenleaf, A.L. (1985). A mutation in the largest subunit of RNA polymerase II alters RNA chain elongation in vitro. J. Biol. Chem. *260*, 13190–13198.

Danan, M., Schwartz, S., Edelheit, S., and Sorek, R. (2012). Transcriptome-wide discovery of circular RNAs in Archaea. Nucleic Acids Res. *40*, 3131–3142.

de la Mata, M., Alonso, C.R., Kadener, S., Fededa, J.P., Blaustein, M., Pelisch, F., Cramer, P., Bentley, D., and Kornblihtt, A.R. (2003). A slow RNA polymerase II affects alternative splicing in vivo. Mol. Cell *12*, 525–532.

Dubin, R.A., Kazmi, M.A., and Ostrer, H. (1995). Inverted repeats are necessary for circularization of the mouse testis *Sry* transcript. Gene *167*, 245–248.

Engreitz, J.M., Pandya-Jones, A., McDonel, P., Shishkin, A., Sirokman, K., Surka, C., Kadri, S., Xing, J., Goren, A., Lander, E.S., et al. (2013). The Xist lncRNA exploits three-dimensional genome architecture to spread across the X chromosome. Science *341*, 1237973.

Glažar, P., Papavasileiou, P., and Rajewsky, N. (2014). circBase: a database for circular RNAs. RNA *20*, 1666–1670.

Goers, E.S., Purcell, J., Voelker, R.B., Gates, D.P., and Berglund, J.A. (2010). MBNL1 binds GC motifs embedded in pyrimidines to regulate alternative splicing. Nucleic Acids Res. *38*, 2467–2484.

Hansen, T.B., Jensen, T.I., Clausen, B.H., Bramsen, J.B., Finsen, B., Damgaard, C.K., and Kjems, J. (2013). Natural RNA circles function as efficient microRNA sponges. Nature *495*, 384–388.

Houseley, J.M., Garcia-Casado, Z., Pascual, M., Paricio, N., O'Dell, K.M., Monckton, D.G., and Artero, R.D. (2006). Noncanonical RNAs from transcripts of the *Drosophila muscleblind* gene. J. Hered. *97*, 253–260.

Ip, J.Y., Schmidt, D., Pan, Q., Ramani, A.K., Fraser, A.G., Odom, D.T., and Blencowe, B.J. (2011). Global impact of RNA polymerase II elongation inhibition on alternative splicing regulation. Genome Res. *21*, 390–401.

Jeck, W.R., Sorrentino, J.A., Wang, K., Slevin, M.K., Burd, C.E., Liu, J., Marzluff, W.F., and Sharpless, N.E. (2013). Circular RNAs are abundant, conserved, and associated with ALU repeats. RNA *19*, 141–157.

Kadener, S., Menet, J.S., Sugino, K., Horwich, M.D., Weissbein, U., Nawathean, P., Vagin, V.V., Zamore, P.D., Nelson, S.B., and Rosbash, M. (2009). A role for microRNAs in the *Drosophila* circadian clock. Genes Dev. *23*, 2179–2191.

Kaida, D., Berg, M.G., Younis, I., Kasim, M., Singh, L.N., Wan, L., and Dreyfuss, G. (2010). U1 snRNP protects pre-mRNAs from premature cleavage and polyadenylation. Nature *468*, 664–668.

Khodor, Y.L., Rodriguez, J., Abruzzi, K.C., Tang, C.H., Marr, M.T., 2nd, and Rosbash, M. (2011). Nascent-seq indicates widespread cotranscriptional pre-mRNA splicing in *Drosophila*. Genes Dev. *25*, 2502–2512.

Khodor, Y.L., Menet, J.S., Tolan, M., and Rosbash, M. (2012). Cotranscriptional splicing efficiency differs dramatically between *Drosophila* and mouse. RNA *18*, 2174–2186.

Kornblihtt, A.R., Schor, I.E., Alló, M., Dujardin, G., Petrillo, E., and Muñoz, M.J. (2013). Alternative splicing: a pivotal step between eukaryotic transcription and translation. Nat. Rev. Mol. Cell Biol. *14*, 153–165.

Lorenz, R., Bernhart, S.H., Höner Zu Siederdissen, C., Tafer, H., Flamm, C., Stadler, P.F., and Hofacker, I.L. (2011). ViennaRNA Package 2.0. Algorithms Mol. Biol. *6*, 26.

Lukiw, W.J. (2013). Circular RNA (circRNA) in Alzheimer's disease (AD). Front. Genet. *4*, 307.

Melamed, Z., Levy, A., Ashwal-Fluss, R., Lev-Maor, G., Mekahel, K., Atias, N., Gilad, S., Sharan, R., Levy, C., Kadener, S., and Ast, G. (2013). Alternative splicing regulates biogenesis of miRNAs located across exon-intron junctions. Mol. Cell *50*, 869–881.

Memczak, S., Jens, M., Elefsinioti, A., Torti, F., Krueger, J., Rybak, A., Maier, L., Mackowiak, S.D., Gregersen, L.H., Munschauer, M., et al. (2013). Circular RNAs are a large class of animal RNAs with regulatory potency. Nature *495*, 333–338.

Osborne, R.J., and Thornton, C.A. (2006). RNA-dominant diseases. Hum. Mol. Genet. *15*, R162–R169.

Pasman, Z., Been, M.D., and Garcia-Blanco, M.A. (1996). Exon circularization in mammalian nuclear extracts. RNA *2*, 603–610.

Raker, V.A., Mironov, A.A., Gelfand, M.S., and Pervouchine, D.D. (2009). Modulation of alternative splicing by long-range RNA structures in *Drosophila*. Nucleic Acids Res. *37*, 4533–4544.

Rodriguez, J., Tang, C.H., Khodor, Y.L., Vodala, S., Menet, J.S., and Rosbash, M. (2013). Nascent-Seq analysis of *Drosophila* cycling gene expression. Proc. Natl. Acad. Sci. USA *110*, E275–E284.

Salzman, J., Gawad, C., Wang, P.L., Lacayo, N., and Brown, P.O. (2012). Circular RNAs are the predominant transcript isoform from hundreds of human genes in diverse cell types. PLoS ONE *7*, e30733.

Salzman, J., Chen, R.E., Olsen, M.N., Wang, P.L., and Brown, P.O. (2013). Cell-type specific features of circular RNA expression. PLoS Genet. *9*, e1003777.

Wang, E.T., Cody, N.A., Jog, S., Biancolella, M., Wang, T.T., Treacy, D.J., Luo, S., Schroth, G.P., Housman, D.E., Reddy, S., et al. (2012). Transcriptome-wide regulation of pre-mRNA splicing and mRNA localization by muscleblind proteins. Cell *150*, 710–724.

Wang, P.L., Bao, Y., Yee, M.C., Barrett, S.P., Hogan, G.J., Olsen, M.N., Dinneny, J.R., Brown, P.O., and Salzman, J. (2014). Circular RNA is expressed across the eukaryotic tree of life. PLoS ONE *9*, e90859.

Yue, S., Serra, H.G., Zoghbi, H.Y., and Orr, H.T. (2001). The spinocerebellar ataxia type 1 protein, ataxin-1, has RNA-binding activity that is inversely affected by the length of its polyglutamine tract. Hum. Mol. Genet. *10*, 25–30.

Zhao, W., and Manley, J.L. (1996). Complex alternative RNA processing generates an unexpected diversity of poly(A) polymerase isoforms. Mol. Cell. Biol. *16*, 2378–2386.